01 Apr 2017

Ballistic Limit Equations for Non-Aluminum Projectiles Impacting Dual-Wall Spacecraft Systems

William P. Schonberg
Missouri University of Science and Technology, wschon@mst.edu

J. Martin Ratliff

Recommended Citation

W. P. Schonberg and J. M. Ratliff, "Ballistic Limit Equations for Non-Aluminum Projectiles Impacting Dual-Wall Spacecraft Systems," *Proceedings of the 14th Hypervelocity Impact Symposium (2017, Canterbury, UK)*, vol. 204, pp. 516-521, Elsevier, Apr 2017.
The definitive version is available at https://doi.org/10.1016/j.proeng.2017.09.750

Available online at www.sciencedirect.com

ScienceDirect

Procedia Engineering 204 (2017) 516–521

Procedia Engineering

www.elsevier.com/locate/procedia

14th Hypervelocity Impact Symposium 2017, HVIS2017, 24-28 April 2017, Canterbury, Kent, UK

Ballistic limit equations for non-aluminum projectiles impacting dual-wall spacecraft systems

William P. Schonberg[a],*, J. Martin Ratliff[b]

[a]*Missouri University of Science and Technology, Rolla, MO 65409, USA*
[b]*Jet Propulsion Laboratory, California Institute of Technology, Pasadena, CA 91125, USA*

Abstract

One of the primary design considerations of earth-orbiting spacecraft is the mitigation of the damage that might occur from an on-orbit MMOD impact. Traditional damage-resistant design consists of a 'bumper' that is placed a small distance away from a spacecraft component or from the wall of the element in which it is housed. The performance of such a multi-wall structural element is typically characterized by its ballistic limit equation (BLE), which defines the threshold particle size that results in a failure of the spacecraft element. BLEs are also key components of any micro-meteoroid/orbital debris (MMOD) risk assessment calculations. However, these assessments often call for BLEs to predict impact response for projectiles made of materials not used in the development of those BLEs. The question naturally arises regarding how close are the predictions of such BLEs when used in impact scenarios involving projectiles made of materials not necessarily considered in their development. In an effort to address this issue, a study was performed with the objective of assessing the validity of the NNO BLE for non-aluminum particles. Particle materials considered included steel, copper, and Al_2O_3 (i.e. particles that are made of materials that are more dense than aluminum). Comparisons are made between actual test results involving these non-aluminum projectiles and the predictions of the NNO BLE. In nearly all cases, the NNO BLE was found not to work very well in the predicting failure / no failure response of these non-aluminum projectiles. A new NNO-type BLE is then developed that can be used to more reliably predict the response of dual-wall systems under the hypervelocity impact of such "heavier" non-aluminum projectiles.

Peer-review under responsibility of the scientific committee of the 14th Hypervelocity Impact Symposium 2017.

Keywords: ballistic limit equation; non-aluminum projectiles; dual-wall structure; orbital debris; risk assessment

---

* Corresponding author. Tel.: +1-573-341-4787; fax: +1-573-341-4729.
E-mail address: wschon@mst.edu

1877-7058 © 2017 The Authors. Published by Elsevier Ltd.
Peer-review under responsibility of the scientific committee of the 14th Hypervelocity Impact Symposium 2017.
10.1016/j.proeng.2017.09.750

1. Introduction

One of the primary considerations of earth-orbiting spacecraft is the anticipation and mitigation of the possible damage that might occur from an on-orbit MMOD impact. Traditional damage-resistant wall design consists of a 'bumper' plate that is placed at a small distance away from a spacecraft component or from the wall of the compartment or element in which it is housed. The bumper protects the spacecraft component by disintegrating the impacting particle to create one or more diffuse debris clouds that travel towards and eventually impact it or its main or inner protective element. The area over which the impulsive loading of these debris clouds is distributed is governed by the manner in which the projectile and bumper fragment, melt, or vaporize, and by the spacing between the bumper and the inner wall or protected element.

The performance of the multi-wall structural element is typically characterized by its ballistic limit equation (BLE), which defines the threshold particle size that would result in its failure as a function of velocity, impact angle, particle density, particle shape, as well as the composition and geometry of the structural element. This failure can be in the form of a perforation (i.e. a hole) in the main or inner wall of the system. BLEs for multi-wall systems are typically drawn as lines of demarcation between regions of inner-wall failure and non-failure in two-dimensional projectile diameter-impact velocity space; when graphically represented, they are often referred to, in this form, as ballistic limit curves (BLCs).

Ballistic limit equations are one of the key components of any micro-meteoroid/orbital debris (MMOD) risk assessment calculations. However, these assessments often call for the BLEs to be used to predict the response of spacecraft components under the impact of projectiles made of materials that were not used in the development of those BLEs. The question naturally arises regarding how close are the predictions of such BLEs when used in impact scenarios involving projectiles made of materials not necessarily considered in their development.

In an effort to address this issue, a study was performed with the objective of assessing the validity of the primarily-aluminum-projectile-based NNO BLE [1] for non-aluminum particles. Particle materials considered included steel, copper, and Al_2O_3 (i.e. particles that are made of materials that are more dense than aluminum). Debris populations having particles with densities approximating these materials are specifically called out in the NASA debris environment model, ORDEM-3 [2].

In this paper we present comparisons between actual test results involving these “heavier” non-aluminum projectiles and the predictions of the NNO BLE. In nearly all cases, the NNO BLE was found not to work sufficiently well in predicting failure / no failure response of these non-aluminum projectiles. Suggestions are then made regarding how the NNO BLE could be adjusted to accommodate the impact of such more dense non-aluminum projectiles. The end product is a new NNO-type BLE that can be used to more reliably predict the response of dual-wall systems under the hypervelocity impact of “heavier” non-aluminum projectiles.

2. Original dual-wall ballistic limit equations

The BLE for a dual-wall structure is known for its characteristic “bucket shape”, which is a direct result of the phenomenological changes in response that occur at different impact velocities, from (nearly) complete projectile fragmentation (near 3 km/s for aluminum-on-aluminum impacts) to complete projectile melt (near 7 km/s for aluminum-on-aluminum impacts). The space between the dual-wall BLE and that of an equal-eight single-wall BLE is a measure of the increase in protection provided by a dual-wall system over that provided by its equal-weight single-wall counterpart.

The dual-wall BLE used by NASA and others to characterize the response of many dual-wall structural configurations is frequently referred to by the spacecraft design community as the New Non-Optimum, or “NNO”, BLE [1]. The equations for the low velocity and high velocity regions of the NNO BLE are written, respectively, as follows:

$$V_n = V_p\cos\theta_p < 3\text{ km/s:} \qquad d_{c,L} = f_L(t_b,t_w,\rho_p,\sigma_w)C_L[(V_p\cos\theta_p)^{-2/3}]^{18/19} \tag{1}$$

$$V_n = V_p\cos\theta_p > 7\text{ km/s:} \qquad d_{c,H} = f_H(t_w,\rho_p,\rho_b,\sigma_w,S)C_H(V_p\cos\theta_p)^{-2/3} \tag{2}$$

In equations (3) and (4), f_L and f_H are functions that contain information regarding the geometry of the particular dual-wall system under consideration, and $C_L=(1/0.6)^{18/19}$ and $C_H=3.918$ are parameters that seek to place the BLE in the most appropriate place on the plot of empirical failure / non-failure data points.

This BLE was developed primarily for aluminum-on-aluminum impacts and for dual-wall configurations with bumpers or shields that are sufficiently thick so as to cause significant fragmentation of an incoming projectile. In order to be able to use the NNO BLE in risk assessments that also used ORDEM-3, the NNO BLE had to be modified to include a higher high-end transition velocity option. A recent study by the NASA Johnson Space Center Hypervelocity Impact Technology (HVIT) group found that a value of 9.1 km/s would be an appropriate high-end transition velocity for steel particles impacting aluminum plates [3]. This option would then engage whenever a risk assessment run called for a calculation involving the impact of a high density particle, such as steel. However, no modifications were made to the low-end transition velocity of the NNO BLE. That is, as encoded in Bumper 3, the latest version of NASA's MMOD risk predictor computer program, it remains at a value of 3 km/s for normal aluminum-on-aluminum impacts as well as for steel-on-aluminum impacts, in spite of some suggested low-end transition values for more dense projectiles offered by Kalinski [4].

The work reported in this paper built on these initial efforts by considering other projectile materials that are more dense than aluminum. This study focused on cooper [5-8], steel [4,7,9-12], and aluminum oxide (Al_2O_3) [4] projectiles impacting all-aluminum dual-wall systems. Other more dense non-aluminum projectiles, such as cadmium, lead, etc., have also been used in previous high-speed impact test programs, but the tests with those projectiles typically involved like-material bumpers, and hence were not considered in this study. Actual test results were compared against the NNO BLE, which subsequently led to further modifications of the NNO BLE so that it could accommodate these more dense projectiles. These modifications included adjustments of both the low-end and high-end transition velocity values as well as some adjustments of the constants used in the low velocity and high velocity region equations.

In order to be able to pool together the wide assortment of test configurations (e.g. widely varying bumper thicknesses, inner wall thicknesses, and stand-off distances in the specimens tested in [4-12]), the NNO BLE was normalized by

- dividing both sides of the $V_n<3$ km/s and $V_n>7$ km/s equations by the terms involving all material and geometric properties, that is, f_L and f_H, respectively. As a result, only the coefficients $C_L=(1/0.6)^{18/19}$ and $C_H=3.918$ and the velocity terms $[(V\cos\theta)^{-2/3}]^{18/19}$ and $(V\cos\theta)^{-2/3}$ remained on the right hand side of the $V_n<3$ km/s and $V_n>7$ km/s equations, respectively.
- multiplying the normalized ballistic limit diameter values obtained in the previous step by another factor to take into consideration the differences in the formulations of f_L and f_H and to smooth out those differences during the normalization process.

In the end, the normalized forms of the NNO BLE in the low- and high-velocity impact regimes were given as follows:

$$V_n < 3 \text{ km/s:} \qquad d_{c,L}^{norm} = \left(\frac{d_{c,L}}{f_L}\right)\sqrt{\frac{f_H}{f_L}} \tag{3}$$

$$V_n > 7 \text{ km/s:} \qquad d_{c,H}^{norm} = \left(\frac{d_{c,H}}{f_H}\right)\sqrt{\frac{f_L}{f_H}} \tag{4}$$

Finally, in the region where $3<V_n<7$ km/s, the normalized NNO BLE was obtained by interpolating between the values of the normalized NNO BLE at $V_n=3$ km/s and at $V_n=7$ km/s. Figure 1 shows plots of the normalized NNO BLE, with and without the high-end transition velocity modification suggested in [3]. Also shown are the test results for steel projectiles impacting a common all-aluminum dual-wall system (2 mm thick aluminum 6061-T6 bumper and 4.83 mm thick aluminum 2219-T87 rear-wall 11.43 cm away from the bumper). This figure displays several interesting features.

First, the region between the two curves are those projectile diameter-impact velocity combinations that the original NNO predicts would not cause inner wall failure (because they lie below the curve). However, the modified NNO BLE (with its new high-end transition velocity – for normal impacts – of 9.1 km/s) predicts that those projectile diameter-impact velocity combinations *would* cause failure to the inner wall of a dual-wall system (because they now lie above the BLE). Not having been completely melted by the impact on the lower density aluminum plate, these higher density steel projectiles still possess enough energy (as well as momentum) to inflict serious damage on the inner wall plate.

Second, both the 0-deg and the 45-deg test results appear on the same plot. And, concurrently, there is no longer a 45-deg BLE curve or a 0-deg BLE curve – there is only a single normalized BLE curve for the particular dual-wall system under consideration that incorporates the effect of impact angle.

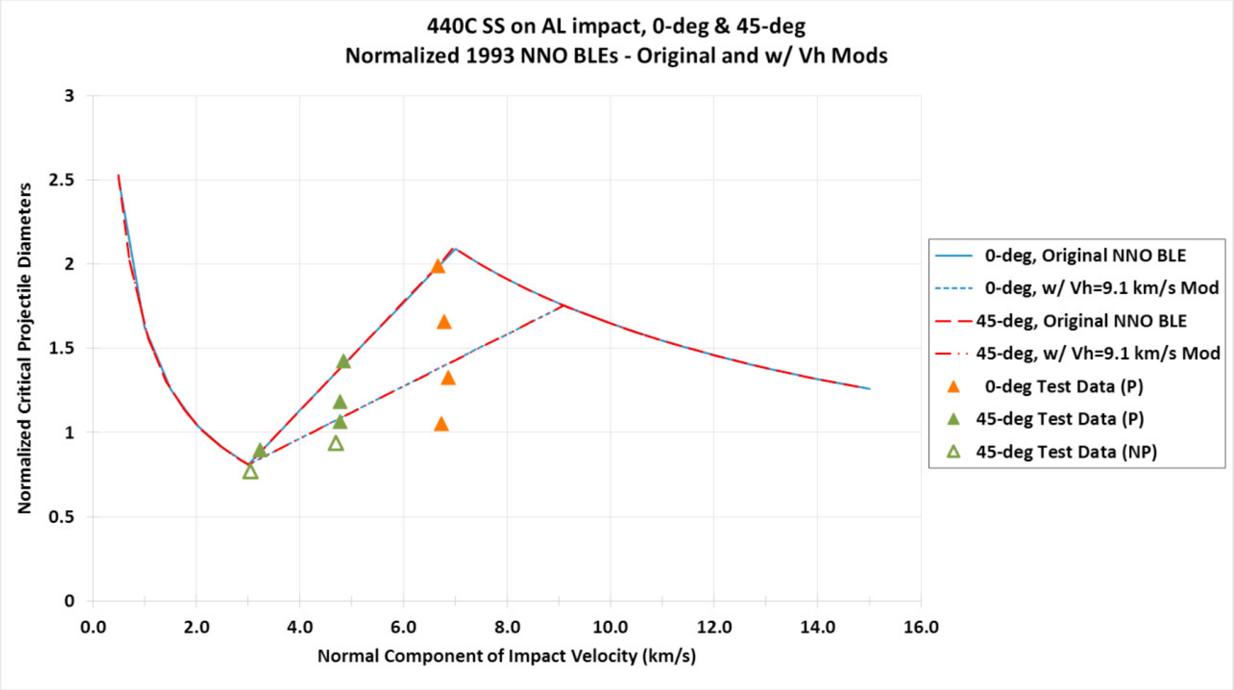

Figure 1. Normalized Impact Test Data Compared Against Normalized Original and Modified NNO BLE

This indicates that the normalization scheme is successful in combining test data at varying trajectory obliquities. It also indicates that whatever modifications are made to the normalized version of the original NNO BLE so that it captures the failure / non-failure characteristics of a normalized test data grouping should transfer back, i.e. the un-normalized versions of modified NNO BLEs should, as a group, be able to do a good job at capturing the failure / non-failure characteristics of individual test data points and groups for their particular geometries, trajectory obliquities, etc.

3. Modified dual-wall ballistic limit equations

It is also clear from Figure 1 that further modifications are needed to the NNO BLE to render it more accurate when predicting the failure / non-failure response of dual-wall aluminum systems. Considering the normalization scheme used thus far, the following parameters are available for adjustment to achieve this goal:

(1) the low-end transition velocity, or V_L,
(2) the high-end transition velocity, or V_H,
(3) the low velocity equation coefficient $C_L = (1/0.6)^{18/19}$, and
(4) the high velocity equation coefficient $C_H = 3.918$.

The first two, V_L and V_H, are linked to changes in response phenomenology that occur as impact velocity is increased, while the second two, C_L and C_H, are curve-fitting parameters that can be adjusted based on the placement of the failure / non-failure data on the plotting grid. Thus, changes to the coefficients C_L and C_H will be made only after the new "anchor points" V_L and V_H are determined.

3.1. Anchor point modification

The impact velocity associated with the high-end transition or anchor point is that at which the impact projectile is fully melted. This velocity can be estimated for each of the projectile materials using a standard 1-D shock physics based calculation (see, e.g. [13]). Table 1 presents the results of those calculations for the impact velocities at which projectile melt is estimated to begin and to be completed (V_{mb} and V_{mc}, respectively) for the materials considered in this study.

Table 1. Velocity Estimates Based on Shock Physics Calculations

	Aluminum	Al_2O_3	Steel	Cooper
V_{mb}	5.40	12.4	7.40	6.45
V_{mc}	6.90	15.9	8.70	7.80

The following key inferences can be drawn from the information in Table 1:

1. The values for the impact velocities at which aluminum projectiles impacting aluminum bumper plates begin to melt and are completely melted as obtained using the 1-D shock and release calculation process agree with the commonly accepted values of 5.5 and 7.0 km/s, respectively. This lends confidence to process and equations used to obtain these values for the other values, except possibly for Al_2O_3.
2. The reason for the above exception for Al_2O_3 is that the velocities at which melt is calculated to begin and to be completed are probably beyond the limits of applicability of the Mie-Gruneisen equation of state.
3. The impact velocity at which melt is completed for steel projectiles impacting aluminum bumper plates (8.7 km/s) is fairly close to the value calculated in [10].

Taking these points and the V_{mb} and V_{mc} values in Table 1 into consideration as well as the goal of developing a single modified BLE for more dense projectile materials (i.e. density greater than ~3.5 gm/cm^3), the following values were proposed for the low-end and high-end transition velocities: $V_L = 5.7$ km/s, $V_H = 9.1$ km/s.

3.2. Coefficient adjustment

As mentioned previously, in addition to modifying the low-end and high-end transition velocities, V_L and V_H, respectively, the two curve-fitting parameters, C_L and C_H, can be modified based on where the normalized failure / non-failure data were to fall on the plotting grid. Figure 2 below show plots of the revised normalized NNO BLE for projectile materials more dense than aluminum, respectively, based on the V_L and V_H values noted above and the following C_L and C_H values: $C_L = (1/0.33)^{18/19}$, $C_H = 3.918$.

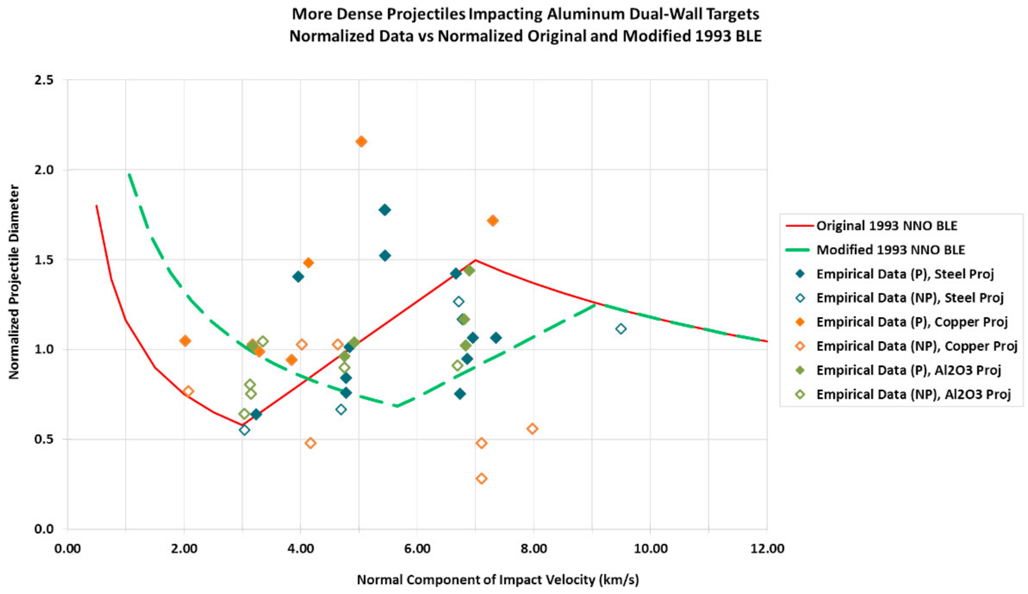

Figure 2 Plots of the Revised and Original Normalized NNO BLEs for Projectile Materials More Dense than Aluminum and Comparisons with Experimental Data

From Figure 2, we can see that these modifications to the NNO BLE create formulae that successfully delineate the boundary between failure / non-failure test results to a much greater extent than does the original all-aluminum BLE. Further, to the extent indicated by the available test data, the adjusted parameters are not particularly sensitive to projectile density within the range of the more dense projectiles (Al_2O_3, steel, copper) that are used to characterize the debris environment in the ORDEM-3 model.

4. Conclusions

This paper presented a summary of the work performed to assess the validity of an existing dual-wall aluminum-projectile-based BLEs for non-aluminum particles. Particle materials considered included steel, copper, and Al_2O_3 (i.e. particles that are made of materials that are more dense than aluminum). In the end, the NNO BLE BLE was found not to work sufficiently well in the predicting the failure / non-failure response of more dense non-aluminum projectiles. This BLE was then modified so that it is now better model the impact response of such more dense non-aluminum projectiles. The results obtained also showed that procedure developed can be used to pool together and directly compare results from a wide range of test conditions and dual-wall configurations.

Acknowledgements

This research was carried out at the Jet Propulsion Laboratory, California Institute of Technology, under a contract with the National Aeronautics and Space Administration.

References

[1] E.L. Christiansen, “Design and Performance Equations for Advanced Meteoroid and Debris Shields”, *International Journal of Impact Engineering*, 14 (1993) 145-156.

[2] E.G. Stansbery, and M.J. Matney, NASA Orbital Debris Engineering Model ORDEM 3.0 - User’s Guide, NASA TP-2014-217370, Johnson Space Center, Houston, Texas, 2014.

[3] M.D. Squire, et al, Joint Polar Satellite System (JPSS) Micrometeoroid and Orbital Debris (MMOD) Assessment, NASA TM-2015-218780, Langley Research Center, Hampton, VA, July 2015.

[4] M. Kalinski, Hypervelocity Impact Analysis of International Space Station Whipple and Enhanced Stuffed Whipple Shields, MS Thesis, Naval Post Graduate School, California, 2004.

[5] R.F. Rolsten, H.H. Hunt, and J.N. Wellnitz, Study of Principles of Meteoroid Protection, Report No. AE-62-0413, General Dynamics Corp., Final Report, Contract NAS-8-875, Marshall Space Flight Center, Huntsville, AL, April 1962.

[6] A.R. McMillan, Experimental Investigations of Simulated Meteoroid Damage to Various Spacecraft Structures, NASA CR-915, Washington, DC, 1968 (also GM-DRL-TR-66-67).

[7] D.P. Hickey, An Experimental Study of High Velocity Impact at Normal And Oblique Incidence on Multiple, Spaced 2024-T3 Aluminum Plates, Douglas Report SM-47873, Douglas Aircraft Company, Santa Monica California, June 1965.

[8] E.L. Christiansen, Meteoroid/Debris Shielding, NASA TP-2003-210788, Johnson Space Center, Houston, Texas, August 2003.

[9] C.J. Maiden, J.W. Gehring, and A.R. McMillan. Investigation of Fundamental Mechanism of Damage to Thin Targets by Hypervelocity Projectiles, GM-DRL-TR-63-225, Santa Barbara, CA, September 1963.

[10] N.C. Elfer, Structural Damage Prediction and Analysis for Hypervelocity Impacts - Handbook, NASA CR-4706, Marshall Space Flight Center, February 1996.

[11] W.P. Schonberg, A.J. Bean, and K. Darzi. Hypervelocity Impact Physics. NASA CR-4343, Marshall Space Flight Center, AL, 1991.

[12] E.L. Christiansen, B. Davis, M. Squire, J. Miller, and D. Lear, NASA NESC High Velocity Impact Study at UDRI: Phase 1**,** February 2013.

[13] W.P. Schonberg, “Debris Cloud Characterization for Hyervelocity Impacts of Single and Multi-material Projectiles on Thin Target Plates”, *Shock and Vibration*, 2 (1995), 273-287.